Talanta 120 (2014) 376–385

Contents lists available at ScienceDirect

Talanta

journal homepage: www.elsevier.com/locate/talanta

The preparation of magnetic molecularly imprinted nanoparticles for the recognition of bovine hemoglobin

Min Zhang, Yuzhi Wang *, Xiaoping Jia, Meizhi He, Minli Xu, Shan Yang, Cenjin Zhang

State Key Laboratory of Chemo/Biosensing and Chemometrics, College of Chemistry and Chemical Engineering, Hunan University, Changsha 410082, PR China

ARTICLE INFO

Article history:
Received 22 October 2013
Accepted 3 December 2013
Available online 18 December 2013

Keywords:
Surface imprinting
Magnetic nanoparticles
Itaconic acid
Bovine hemoglobin

ABSTRACT

The protein imprinted technique combining surface imprinting and nano-sized supports materials is an attractive strategy for protein recognition and rapid separation. In this work, we imprinted bovine hemoglobin (BHb) on magnetic nanoparticles. With itaconic acid (IA) and acrylamide (AAm) as the monomers, the experiment was carried out in aqueous media via surface-imprinting technique. The effects of initial concentration and adsorption time over the adsorption capacity of both imprinted and non-imprinted nanoparticles were analyzed. The maximum adsorption capability of imprinted nanoparticles was found to be 77.6 mg g^{-1}, which was 3.1–4.3 times higher than that of the non-imprinted nanoparticles prepared at the same conditions. This resulted in the successful formation of imprinting cavities. Moreover, in selective adsorption experiment and competitive batch rebinding test, imprinted nanoparticles exhibited a high specific recognition of the template protein over the non-imprinted protein.

1. Introduction

Molecular imprinting has been widely recognized as a potential technique for the synthesis of tailor-made recognition materials by the formation of a polymer network around a template molecule. This is mainly because molecularly imprinted polymers have advantages like specific recognition, high stability, low cost and reusability. To date, molecular imprinting has proven successful in many areas, such as biosensors [1–5], separation [6–8], catalysis [9] and drug delivery [10]. But it is worth noting that these achievements were mainly gained by the imprinting for small molecules, such as herbicides, metal ions, amino acids and so on. The imprinting of biological macromolecules and proteins still remains challenging. First, due to the water solubility and sensitive structural nature of biomacromolecules, imprinting is limited to the water environment, which greatly limits the selection of functional monomer. Second, for large template molecules, high crosslink densities could lead to a slow mass transfer rate, and in the worst case, the template may entrap into the polymer network permanently. Third, there are more functional groups which can interact with functional monomer on the biomacromolecules. And they can cause high nonspecific adsorption. In order to overcome these difficulties, researchers made a lot of efforts in this respect, for example, surface imprinting [11–20], epitope which adopts a fragment of the original macromolecular target as a template [21,22], and moderately cross-linked hydrogels [23–26]. Among these, surface molecular imprinting technique has been widely used in the imprinting process of protein molecules in recent years. Because it is to take certain measures to limit almost all the binding sites formed on the surface, they can have a good accessibility, which can benefit the removal and rebinding of the template molecules.

Usually the supports used in surface molecular imprinting technique are silica beads [14,15], chitosan resins [27–29], and polymer particles [16]. For years now, magnetic nanoparticles as supports have attracted more and more attention because of their unique physical and chemical properties such as large specific surface area, easy to separate from the reaction medium and high mass transfer rate. But the magnetic particles are easily agglomerated. In order to make them disperse in the reaction system more easily, two modification methods were widely used: silylation modification and surfactant modification. Of the two, silylation modification is the most commonly used. In addition, there are no polymerizable groups above the magnetic particles. It is bad for surface molecular imprinting. But for the magnetic particles modified by silicon, we can easily introduce hydroxyl, carboxyl, amino and other functional groups by the sol–gel process [30]. In this way, the loci which can interact with biological macromolecules such as protein will increase to a great extent and the imprinting effect will be better. Qingqing Gai et al. [11,12] synthesized bovine serum albumin (BSA) and lysozyme (Lyz) surface-imprinted magnetic polymer successfully, based on the atomic transfer radical polymerization (ATRP) method.

Hemoglobin (Hb) is well known for its function in the vascular system of animals, being a carrier of oxygen and also aids in the

* Corresponding author. Tel.: +86 731 88821903; fax: +86 731 88821848.
E-mail address: wyzss@hnu.edu.cn (Y. Wang).

0039-9140/$ - see front matter © 2013 Elsevier B.V. All rights reserved.
http://dx.doi.org/10.1016/j.talanta.2013.12.004

transport of carbon dioxide and regulates the pH of blood [31]. It comprises four molecular subunits, and structural changes in any of the four molecular subunits can result in the manifestation of hereditary diseases, sickle cell anemia, thalassemia and so on. Therefore, the enrichment, the separation and the analysis of hemoglobin have important significance. Bovine hemoglobin (BHb) shares 90% amino acid sequence homology with human hemoglobin [32], so we usually choose bovine hemoglobin as the template protein in the process of research. Although there have been some reports on bovine hemoglobin molecular imprinting technique, but not more. This is mainly because bovine hemoglobin has a larger size and a more flexible conformation compared to lysozyme, which is usually used as template protein. Ayşegül Uysal and copartners [24] fabricated the hemoglobin-imprinted hydrogels by using *N*-*t*-butylacrylamide (TBA), acrylamide (AAm) and itaconic acid (IA) monomers, and the maximum adsorption capacity of the obtained gel is 12.4 mg g^{-1} dry gel. Xiaoping Jia et al. [17] imprinted bovine hemoglobin over silica-modified Fe_3O_4 nanoparticles with dopamine as functional monomer and crosslinking agent. The MIP is simple to prepare and easy to separate, but the adsorption capacity is a little small, only 4.65 ± 0.38 mg g^{-1}. Considering all these above, we proposed a novel strategy to imprint BHb.

Itaconic acid (IA) can easily copolymerize and provide polymer chains with carboxylic side groups, which are highly hydrophilic and are able to form hydrogen bonds with the corresponding groups [33]. So far, IA was sometimes used for the imprinting of small molecules. For example, Baoyu Huang et al. [34] prepared monolithic molecularly imprinted polymer for the chiral separation of neurotransmitters and their analogs with IA or MAA as the monomer, respectively. Coincidentally, Lopez et al. [35] synthesized molecularly imprinted polymer with IA or MAA as the monomer, respectively, also, to extract indole alkaloids from Catharanthus roseus extracts. In terms of protein imprinting, only Ayşegül Uysal and copartners [24] once fabricated the hemoglobin-imprinted hydrogels using *N*-*t*-butylacrylamide (TBA), acrylamide (AAm) and itaconic acid (IA) monomers. In this paper, we tried to use it as the co-monomer in the surface imprinting technique.

In this study, surface imprinting of bovine hemoglobin was conducted with vinyl modified magnetic nanoparticles as supports, itaconic acid and acrylamide as functional co-monomers, and N,N′-methylenebisacrylamide as a cross-linker. The Fe_3O_4 nanoparticles were prepared by the coprecipitation method, modified by organic silicon, and then coated with a thin MIPs film. Here we chose acrylamide as the basic monomer. Among all the applied functional monomers at present, NH_2-group of acrylamide can form strong hydrogen bonds in polar solvents, while the carboxyl functional groups of acrylic monomers could interact with the NH_2-group of proteins in the form of ionic bond. So acrylamide and acrylic acid monomers are the two kinds of most commonly used functional monomers. Compared with acrylic monomers, the NH_2-group of acrylamide will not be ionized in the water. So it is more practical [33]. The composition and morphology of the resultant magnetic molecularly imprinted nanoparticles were investigated by X-ray diffraction (XRD), Fourier transform infrared spectrometry (FT-IR), field emission scanning electron microscope (FESEM), thermogravimetric analysis (TGA), vibrating sample magnetometer (VSM), and the adsorption and recognition performance of MIP were discussed through batch rebinding tests, adsorption kinetics, selective adsorption experiments, and competitive batch rebinding tests.

2. Experimental section

2.1. Reagents and instruments

All reagents used were of at least analytical grade and without further purification. Acrylamide, N,N-methylenebisacrylamide (MBAAm) and ammonium persulfate (APS) were supplied from Institute of Fucheng Chemicals (Tianjin, China). Tetraethyl silicate (TEOS) was purchased from Xilong chemistry Co. Ltd. (Shantou, China). 3-(Trimethoxysilyl)-Propyl Methacrylate (γ-MPS) was purchased from Adamas Regent Co. Ltd. N,N,N′,N′-tetramethylenediamine (TEMED) and itaconic acid (IA) were purchased from Aladdin chemistry Co. Ltd. (Shanghai, China). Bovine hemoglobin (BHb, pI 6.9, MW 64.5 kDa), bovine serum albumin (BSA, pI 4.9, MW 66.0 kDa), ovalbumin (OVA, pI 4.7, MW 43.0 kDa) and lysozyme (Lyz, pI 11.2, MW 14.4 kDa) were obtained from DingGuo Biotech (Beijing, China). PB buffer solution (20 mmol L^{-1}, pH 6.2, ionic strength 0.1 M) was used as the working medium.

UV-2450 UV–vis spectrophotometer (Shimadzu, Japan); FT-IR spectrometer (PerkinElmer, USA); JSM-6700F field emission scanning electron microscopy (JEOL, Japan); STA 409 thermal gravimetric analyzer (Netzsch, Germany); EV 11 Vibrating Sample Magnetometer (MicroSense, USA); incubator shaker (QYC 200; FuMa Experimental Equipment Co. Ltd., Shanghai, China); Ultrapure water instrument (RM 220; LiDe Experimental Equipment Co. Ltd, Shanghai, China).

2.2. Preparation of Fe_3O_4 Nanoparticles

Fe_3O_4 nanoparticles were prepared by the coprecipitation method with a little modification [36]. 5 g of $FeCl_3 \cdot 6H_2O$ was dissolved in 30 mL of water, then 1 mL hydrazine hydrate and 2 g $FeSO_4 \cdot 7H_2O$ were added to the solution in sequence. After being dissolved thoroughly, 10 mL 25 vol% ammonium hydroxide was poured into the solution quickly under violent stirring, then added drop by drop until pH=9. The reaction was maintained for 30 min at room temperature. Soon when the temperature was elevated to 80 °C, the mixture was cured for 1 h. The black superparamagnetic Fe_3O_4 nanoparticles were then separated from the reaction system by a magnet and washed with ultrapure water until the washing solution was neutral. Finally the particles were washed with anhydrous ethanol three times and dried in a vacuum drying oven at 70 °C for 24 h.

2.3. Synthesis of functionalized magnetic nanoparticles

The method of modified Fe_3O_4 nanoparticles with silicon was carried out as Ref. [17]. As is known, the existence of a double bond can assure the tight growth of MIPs film on the surface of Fe_3O_4@SiO_2 nanoparticles [13]. So the Fe_3O_4@SiO_2 nanoparticles were modified with γ-MPS by the sol–gel method according to Ref. [13], but with a little adjustment. Briefly, γ-MPS (600 μL) were dispersed in 120 mL ultrapure water containing 10% acetic acid through mechanical stirring for 5 h. Then, Fe_3O_4@SiO_2 nanoparticles (750 mg) were added into this solution. The reaction proceeded 6 h at 60 °C under continuous mechanical stirring. The resulting product was obtained by magnetic separation and then washed with ultrapure water until the washing solution was pH=7. The Fe_3O_4@MPS nanoparticles were dried in a vacuum drying oven at 60 °C for 24 h.

2.4. Synthesis of BHb-imprinted nanoparticles

The magnetic molecularly imprinted nanoparticles for the selective recognition of bovine hemoglobin (BHb) was prepared by the surface-imprinting technique using itaconic acid (IA) and acrylamide (AAm) as monomers, and MBAAm as cross-linker. In addition, ammonium persulfate and TEMED were used as the initiator and accelerator, respectively. The different AAm/IA ratios were investigated, and the mass of the monomers used is shown in Table 1.

Table 1
Preparative composition of different MIPs.

MIPs	BHb (mg)	AAm (mg)	IA (mg)	MBAAm (mg)	APS (20%)	TEMED (20%)
MIP1	32	32	27.2	16	50μL	50μL
MIP2	32	32	13.6	16	50μL	50μL
MIP3	32	32	5.44	16	50μL	50μL
MIP4	32	32	0.544	16	50μL	50μL
MIP5	32	32	0	16	50μL	50μL
NIP1		32	27.2	16	50μL	50μL
NIP2		32	13.6	16	50μL	50μL
NIP3		32	5.44	16	50μL	50μL
NIP4		32	0.544	16	50μL	50μL
NIP5		32	0	16	50μL	50μL

For the coating of bovine hemoglobin-imprinted film, the modified nanoparticles (200 mg), AAm (32 mg), IA (0–27.2 mg) and MBAAm (16 mg) were dissolved in 40 mL of phosphate buffer (20 mmol L^{-1}, pH 6.2, ionic strength 0.1 M) and mixed thoroughly ultrasonically. Subsequently, bovine hemoglobin (32 mg) was added to the mixture. After prepolymerization which was conducted by rocking in a shaker for 1 h, the solution was deoxygenated by purging with nitrogen for 15 min. Soon 50 μL of APS (20% w/v) and 50 μL of TEMED (20%v/v) were injected to the mixture to initiate the polymerization reaction, which was incubated at room temperature for 24 h. After that, the Fe_3O_4@MIPs were washed with 10% (v/v) acetic acid containing 10% (w/v) SDS solution to remove the embedded template till the washed solution has no absorption at 406 nm. Then they were washed with ultrapure water to remove the entrapped eluent. Finally, the particles were dried in a vacuum drying oven for further use. The control nanoparticles (Fe_3O_4@NIPs) were prepared in the same way and washed in the same way too, but without template bovine hemoglobin.

2.5. Batch rebinding tests

BHb-MIPs (NIPs) (10 mg) accurately weighed were placed into a 2-ml centrifuge tube. Then 1 mL of the protein solution with different initial concentrations was added into each centrifuge tube. The solution was shaken at room temperature for 3 h. The concentration of bovine hemoglobin in the supernatant solution was measured using the UV-spectrometer at 406 nm detection wavelength. The experimental data was presented as the adsorption capacity per unit mass (mg) of the nanoparticles, and the adsorption capacity (Q) was calculated from the following equation:

$$Q = \frac{(C_i - C_f) \times V}{m}$$

In the above equation, C_i (mg/mL) is the initial concentration of protein solution, C_f (mg/mL) is the final protein concentration of the supernatant solution, V (mL) is the volume of the initial solution and m (mg) is the mass of BHb-MIPs (NIPs).

The specific recognition property of the imprinted particles is assessed by the imprinting factor (IF), which is defined as

$$IF = \frac{Q_{MIP}}{Q_{NIP}}$$

where Q_{MIP} is the adsorption capacity of the protein or analog on the imprinted particles, and Q_{NIP} is the adsorption capacity on the non-imprinted particles.

The Langmuir isotherm was applied for the isotherm equilibrium adsorption:

$$\frac{C_e}{Q_e} = \frac{K}{Q_{max}} + \frac{C_e}{Q_{max}}$$

where C_e is the concentration of BHb in the final equilibrium solution (mg mL^{-1}), Q_{max} and Q_e are the theoretical maximum adsorption capacity and the experimental adsorption capacity to the template protein of the MIP or NIP particles, respectively (mg g^{-1}), and K is the dissociation constant (mg mL^{-1}).

2.6. Adsorption kinetics study

The adsorption kinetics is carried out to study how the adsorption capability changes over time. The adsorption experiments were performed with an initial BHb concentration of 1.0 mg/mL and other factors were the same as the single-protein batch rebinding tests. Take samples at regular time intervals for UV–vis analysis to determine the BHb concentrations. The tests were conducted in triplicate.

2.7. Selective adsorption experiments

In the selectivity experiments, three kinds of proteins (BSA, ovalbumin, and lysozyme) were chosen as the reference substrates to investigate the selectivity to the template protein. For the separative adsorption experiments, the different protein solutions (each with a concentration of 1.0 mg mL^{-1}) were applied to bind with the MIP and NIP particles, respectively. The resulting concentrations of BSA, ovalbumin and lysozyme were measured by the UV-2450 separatively.

2.8. Competitive batch rebinding tests

In the competitive batch rebinding tests, the selectivity of the imprinted particles was studied in a binary BHb–BSA solution. The polymeric particles were subjected to a binary protein mixture of BHb and BSA with individual initial concentrations of 1.0 mg/mL. The adsorption mixture was rotary mixed for 24 h. The final concentration of the two proteins was determined by UV/vis spectrophotometry. Moreover, for the mixed adsorption experiments, ovalbumin was chosen as the competitive protein. The adsorption was performed within a protein mixture (containing 1.0 mg mL^{-1} BHb and 1.0 mg mL^{-1} OVA). Ten microliter of the mixed solution, before and after the adsorption, was used for sodium dodecyl sulfate polyacrylamide gel electrophoresis (SDS-PAGE) analysis with 12% polyacrylamide separating gel (Mini-protean-3, Bio-Rad).

In the study of the real sample, the bovine calf serum was used as the BHb source. A mass of 30 mg imprinted and non-imprinted nanoparticles was applied to adsorb the BHb from bovine calf serum. After the adsorption, the particles were washed with SDS-acetic acid (10% w/v:10% v/v) solution. The eluates were desalted, and then 10 μL of the sample was used for sodium dodecyl sulfate polyacrylamide gel electrophoresis (SDS-PAGE) analysis with 12% polyacrylamide separating gel (Mini-protean-3, Bio-Rad).

3. Results and discussion

3.1. Synthesis of BHb-imprinted magnetic nanoparticles

The synthesis process of the magnetic molecularly imprinted nanoparticles usually included four parts: synthesis of the superparamagnetic Fe_3O_4 nanoparticles, modification of the superparamagnetic Fe_3O_4 nanoparticles, coating MIPs film onto the modified nanoparticles, and removal of the template protein. Our study is not exceptional also. The overall synthetic process of Fe_3O_4@MIPs is illustrated in Fig. 1. First, Fe_3O_4 nanoparticles were prepared by the coprecipitation of Fe^{2+} and Fe^{3+}. As we all

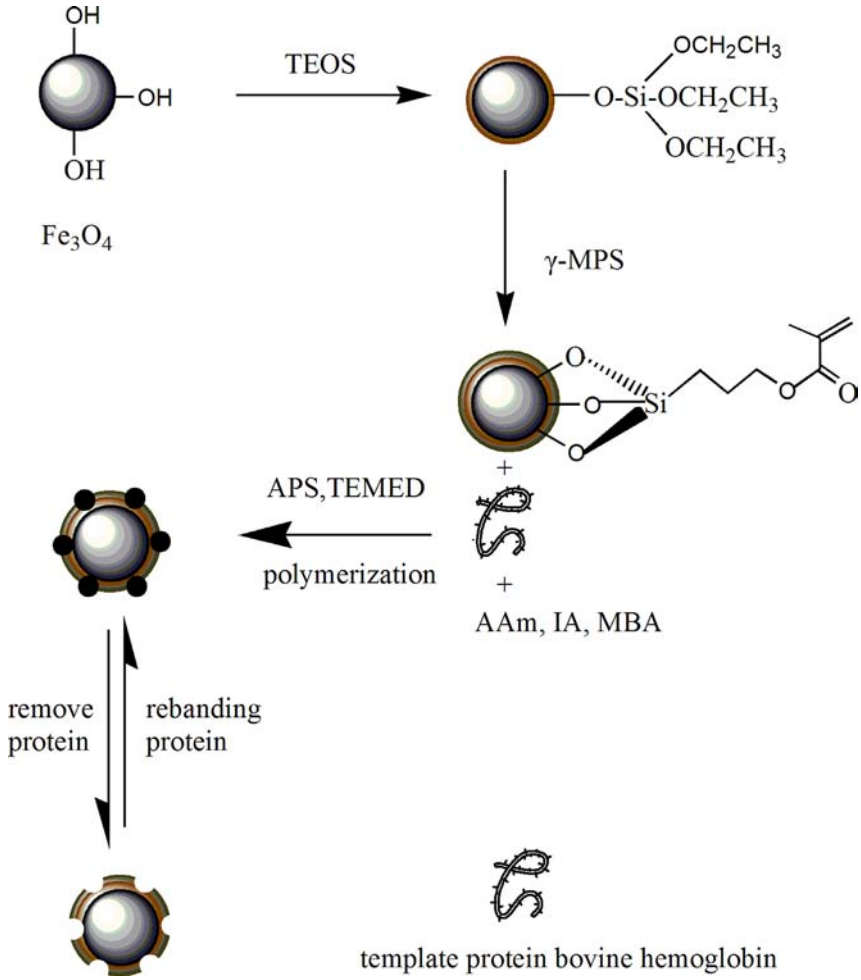

Fig. 1. The schematic illustration of the preparation of BHb–MIPs.

know, Fe_3O_4 nanoparticles can be easily oxidized to γ-Fe_2O_3. So in the second step we modify the Fe_3O_4 nanoparticles with TEOS. And this was conducted by a sol–gel process. The principle is explained in detail in Ref. [17]. The silica-shell coating on the surface of Fe_3O_4 nanoparticles not only can prevent the oxidation of Fe_3O_4 but also could improve the corrosion resistance, chemical stability and effectively reduce the aggregation of Fe_3O_4 nanoparticles in the liquid. What is more important, surface silanol groups could offer many possibilities for further surface modification, such as the introduction of hydroxyl, carboxyl. In terms of this, to ensure the tight growth of MIPs film, double bond was introduced onto the surface of SiO_2 shell using γ-MPS. Finally, MIPs thin films were coated onto the silica-modified Fe_3O_4 nanoparticles by a surface imprinting process. In this research, a new type of MIPs was prepared through the copolymerization AAm and IA. And the ratio of AAm/IA was investigated. The adsorption capacities of the imprinted and non-imprinted nanoparticles which were prepared with different AAm/IA ratios are shown in Fig. 2. We see that group 4 is better than the other four groups undoubtedly. It is interesting to find that with the change in the addition amount of IA, the adsorption capability of NIPs changed little, but this change had a large impact on the adsorption capability of MIPs. This may be the result of the joint effect of electrostatic attraction and space steric hindrance. The role of itaconic acid can be viewed from two perspectives. On one side, the addition of itaconic acid can provide polymer chains with carboxylic side groups, which are able to form hydrogen bonds with corresponding groups of the template protein. On the other side, the over-addition of it will lead to a large steric hindrance, thus reducing the adsorption capability. So looking for a suitable amount on it is very important. MIP 1–3 were synthesized with a higher addition amount of IA, so the

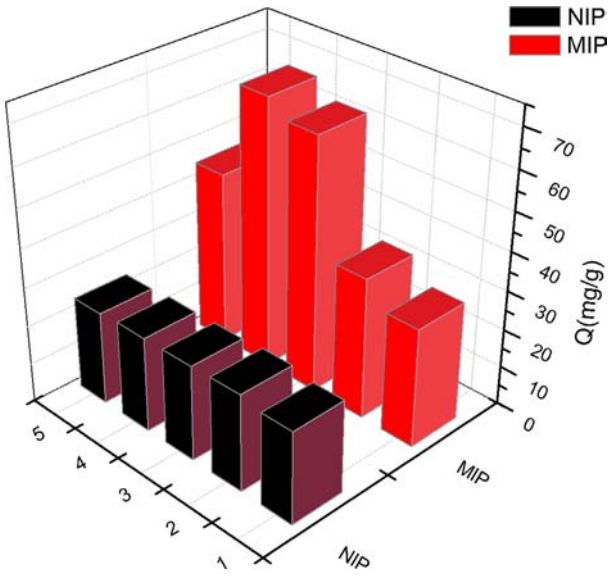

Fig. 2. The adsorption capacities of the imprinted and non-imprinted nanoparticles with different AAm/IA ratio. Adsorption conditions: $V=1$ mL, $m_{MIPs}=m_{NIPs}=10$ mg, $C_{BHb}=1.0$ mg mL^{-1}, $T=25$ °C, $t=24$ h, pH=6.2. The numbers 1, 2, 3, 4, 5 labeled in the figure correspond to Table 1.

space steric hindrance showed more obviously. And this is the reason why they showed lower adsorption capacity. So the optimal recipe was the modified nanoparticles (200 mg), AAm (32 mg), and IA (0.544 mg). The kind of eluent was also investigated in this study. 0.5 M NaCl and SDS-acetic acid (10% w/v:10% v/v) were used in the process of elution. The results indicated that SDS-acetic acid (10% w/v:10% v/v) has a better elution effect. So we choose it as the eluent in following experiments.

3.2. Characterization of BHb imprinted nanoparticles

XRD patterns for the synthesized magnetic nanoparticles are shown in Fig. 3. In the 2θ range of 10°–80°, the X-ray diffraction peaks for Fe_3O_4 (2θ=35.5°, 57.0°, and 62.6°) can be clearly observed on all the four samples and the X-ray diffraction peaks for Fe_3O_4 (2θ=30.1°, 43.1°, 53.4°) can be identified with careful observation. These peak positions were indexed as (220), (311), (400), (422), (511), and (440) according to the order from small to large, respectively (JCPDS Card: 019-0629). The XRD patterns revealed that the synthesized process did not change the crystalline phase of Fe_3O_4. But, it was not sufficient to exclude the existence of γ-Fe_2O_3. However, the magnetic properties of γ-Fe_2O_3 are similar to Fe_3O_4, so there was no negative impact on the following experiments whether γ-Fe_2O_3 was contained in the samples or not.

The FT-IR spectroscopy measurements were used to confirm whether the modification of Fe_3O_4 was successful (as shown in Fig. 4). The presence of Fe_3O_4 was confirmed by the characteristic peak of Fe–O at 589.88. The wide and strong peak at 1103.49 and the peak at 474.67 were attributed to the Si–O–Si asymmetric stretching vibration and bending vibration, respectively, indicating the formation of silicon shell. It was notable that the Fe_3O_4@MPS showed a strong peak at 1630.84 cm^{-1} corresponding to the carbonyl group of γ-MPS. The reason why the peak appeared at this wave number is because the double bond and carbonyl group form a conjugate structure, which lead to the absorption peak of carbonyl group moving to a low wave number; at the same time, the intensity increased obviously. Through the above analysis, it is easy to know that γ-MPS was modified to the nanoparticles successfully.

FESEM images of Fe_3O_4, Fe_3O_4@SiO_2, Fe_3O_4@MPS, Fe_3O_4@MIPs and Fe_3O_4@NIPs are provided in Fig. 5. From the FESEM images, we can see that all of the particles appear to be nanosized and roughly spherical in shape. Fig. 5A shows the FESEM image of Fe_3O_4. We can see that Fe_3O_4 particles were seriously conglomerated after the drying process. The mean diameter of Fe_3O_4 is about 20 nm. Fig. 5B shows the FESEM image of Fe_3O_4@SiO_2, while its diameter ranged from 300 nm to 600 nm. The larger size reveals that the silica shell was coated on the surface of Fe_3O_4 successfully. Fig. 5C, Fig. 5D and Fig. 5E show the FESEM images of Fe_3O_4@MPS, Fe_3O_4@MIPs and Fe_3O_4@NIPs respectively. Their sizes have no

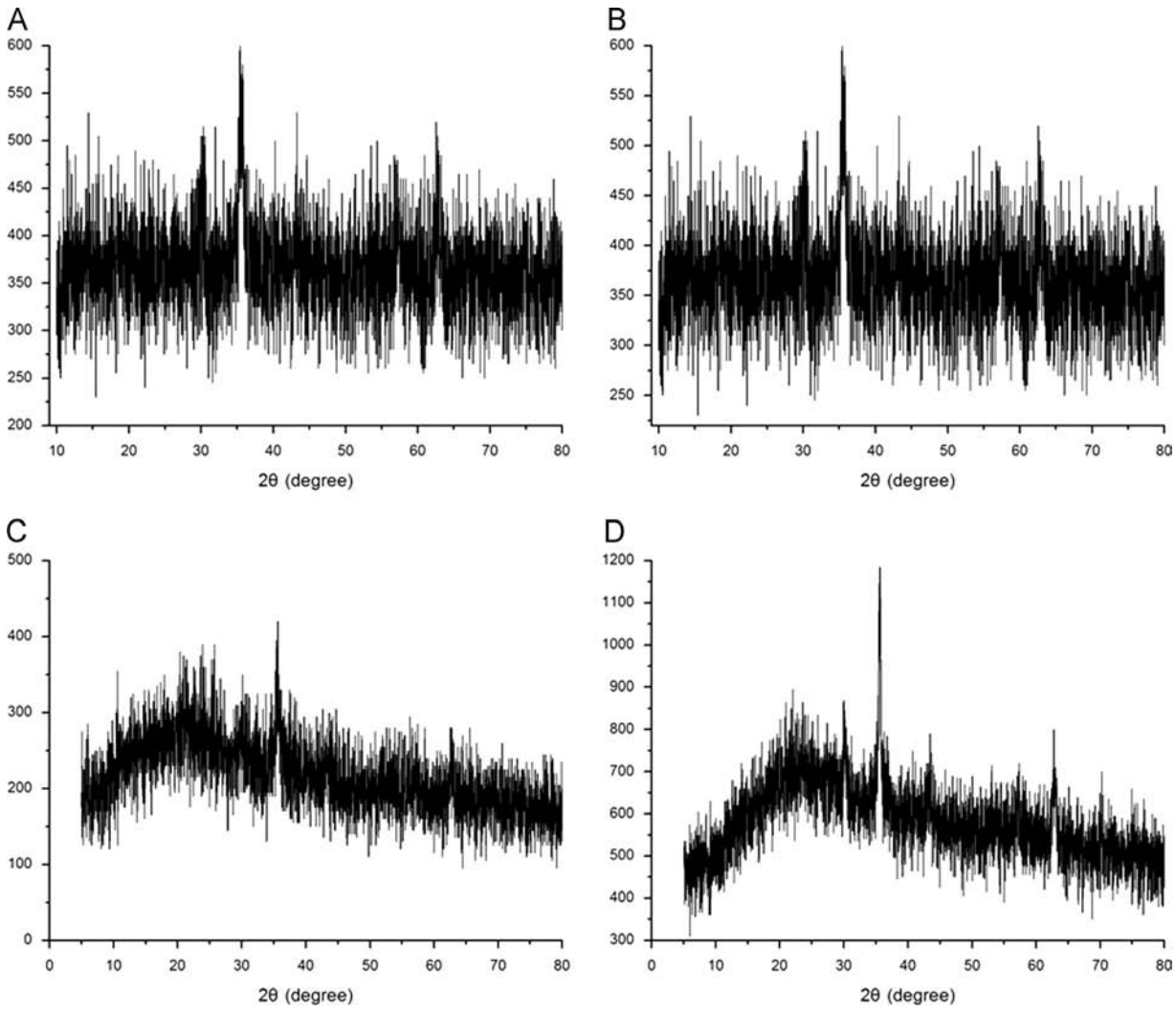

Fig. 3. X-ray diffraction patterns of Fe_3O_4 nanoparticles (a), Fe_3O_4@SiO_2 nanoparticles (b), Fe_3O_4@MPS nanoparticles (c) and Fe_3O_4@MIPs nanoparticles (d).

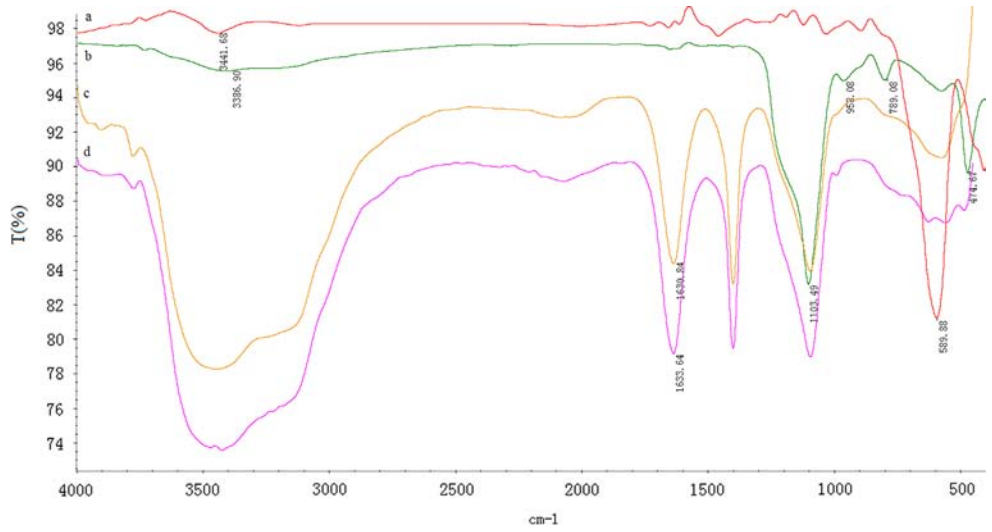

Fig. 4. FT-IR spectra of Fe_3O_4 nanoparticles (a), Fe_3O_4@SiO_2 nanoparticles (b), Fe_3O_4@MPS nanoparticles (c) and Fe_3O_4@MIPs nanoparticles (d).

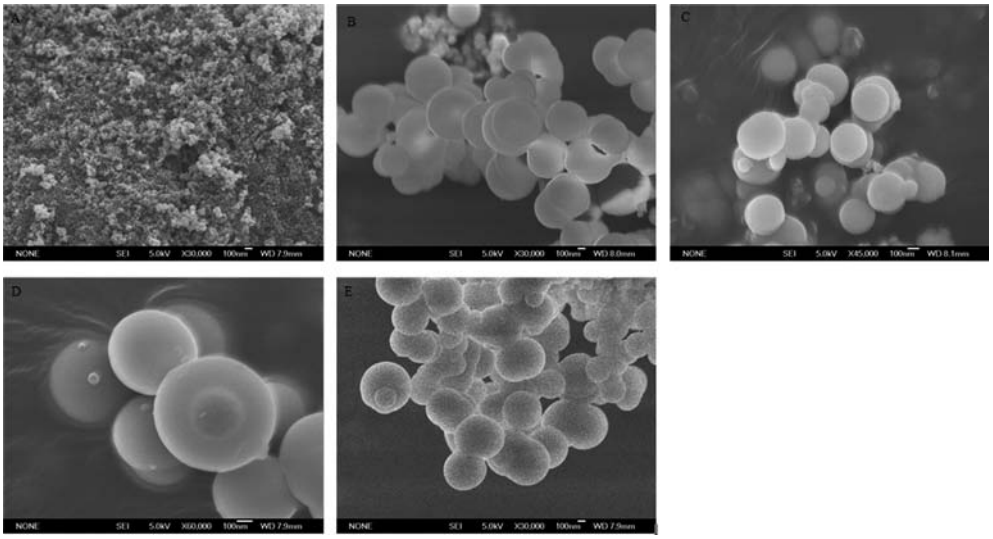

Fig. 5. FESEM images of Fe_3O_4 nanoparticles (A), Fe_3O_4@SiO_2 nanoparticles (B), Fe_3O_4@MPS nanoparticles (C), Fe_3O_4@MIPs nanoparticles (D) and Fe_3O_4@NIPs nanoparticles (E).

obvious change compared to Fe_3O_4@SiO_2. This means the modified layers were very thin.

TGA analysis was employed to further study the relative composition of the magnetic core and the organic shell of the magnetic nanoparticles. As shown in Fig. 6, when the temperature was changed from room temperature to 600 °C, the weight loss of Fe_3O_4@MPS was approximately 11.0%, while the decrease of solvent or water in weight was 3.5% at 180 °C, and the other decrease in weight was 7.5% at 200–600 °C (Fig. 6a). For Fe_3O_4@-MIPs, the weight loss was 19.0% at 600 °C, while the decrease of solvent or water in weight was about 3.3% at 180 °C, and the other decrease in weight was approximately 15.7% for the decomposition of imprinted coatings at 180–600 °C (Fig. 6b). Therefore, the content of magnetite and silica of MIP nanoparticles was about 81.0%. If the mass retention of Fe_3O_4@MPS at 600 °C is used as the reference, there exists ~8.0 wt% difference in the weight retentions at 600 °C between Fe_3O_4@MPS and Fe_3O_4@MIPs. It indicated that the method employed for MIP coating in this work was excellently effective. The grafting yield of MIP coating to Fe_3O_4 @MPS was ~8.0 wt%.

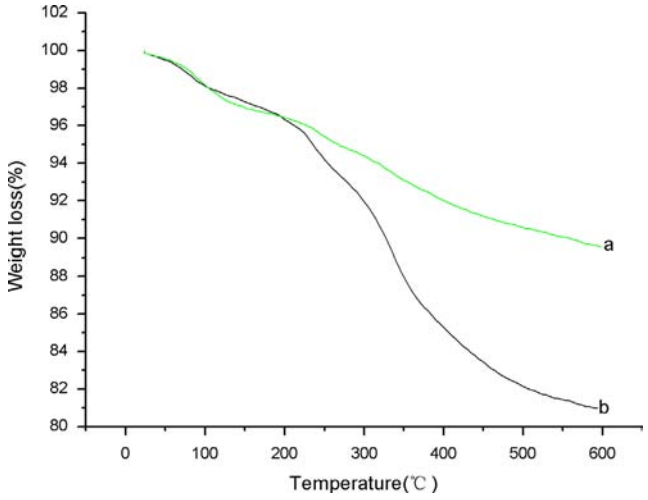

Fig. 6. TGA curves of Fe_3O_4@MPS nanoparticles (a) and Fe_3O_4@MIPs nanoparticles (b).

Magnetism is an important feature of magnetic materials. Sufficient magnetism can ensure that materials separate from liquid medium quickly in practical application. Therefore, VSM was employed to study the magnetic properties of the nanoparticles at room temperature. The magnetic hysteresis loops of Fe_3O_4 and Fe_3O_4@MIP are illustrated in Fig. 7. The saturation magnetization of Fe_3O_4 and Fe_3O_4@MIPs was 32.35 emu g^{-1} and 72.44 emu g^{-1} respectively. The saturation magnetization of Fe_3O_4@MIPs decreased compared with that of Fe_3O_4. This result is expected, caused by the shielding effect of the silica coating and the MIP shell layer on the surface of Fe_3O_4 [17]. Nevertheless, the saturation magnetization value of Fe_3O_4@MIPs nanoparticles was still much higher than those of core–shell magnetic nanoparticles reported in the literatures [17–19]. And in the process of experiment, they can be separated from the suspension quickly. This we can know from Fig. 7B.

3.3. Batch rebinding tests

Fig. 8 is the batch rebinding curve of BHb on Fe_3O_4@MIPs nanoparticles and Fe_3O_4@NIPs nanoparticles. We studied the adsorption capacities of MIPs and NIPs at different initial BHb concentrations, ranging from 0.1 mg/mL to 1.8 mg/mL. Obviously, the MIPs exhibited much higher BHb loadings than the NIPs. When the initial BHb concentration is greater than 1.0 mg/mL, the adsorption capacity of MIPs almost reached a constant value of ~77.6 mg/g. While for NIPs, when the initial BHb concentration is greater than 0.2 mg/mL, the increase of the adsorption quantity is not very obvious. This phenomenon proved the existence of imprinting cavities. Fit the data to the Langmuir equation yield a good linearity for Fe_3O_4@MIPs (R^2=0.9945). According to the equation, the equilibrium constant (K) and the theoretical maximum adsorption capacity (Q_{max}) were calculated to be 0.0146 mg/mL and 77.7 mg/mL, respectively.

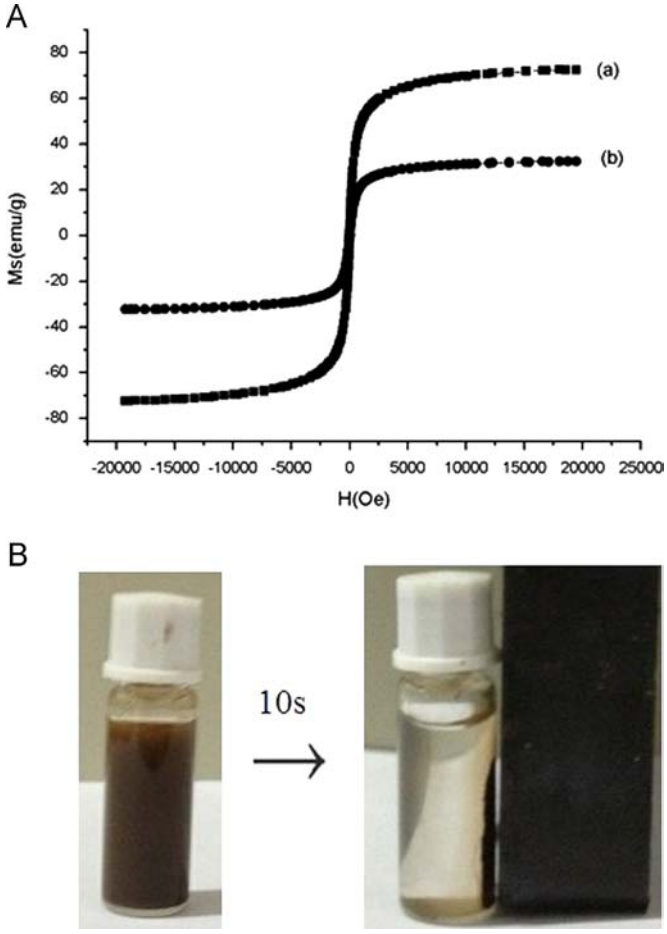

Fig. 7. Magnetic hysteresis loops of Fe_3O_4 nanoparticles A (a), Fe_3O_4@MIPs nanoparticles A (b), and the magnetic response of Fe_3O_4@MIPs to external magnetic field (B).

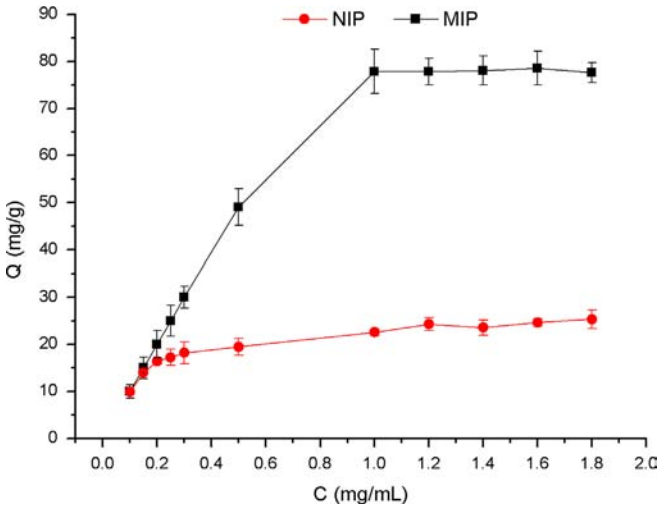

Fig. 8. Batch rebinding curves of BHb on Fe_3O_4@MIPs nanoparticles and Fe_3O_4@NIPs nanoparticles. Adsorption conditions: V=1 mL, m_{MIPs}=m_{NIPs}=10 mg, C_{BHb}=0.1–1.8 mg mL^{-1}, T=25 °C, t=24 h, pH=6.2.

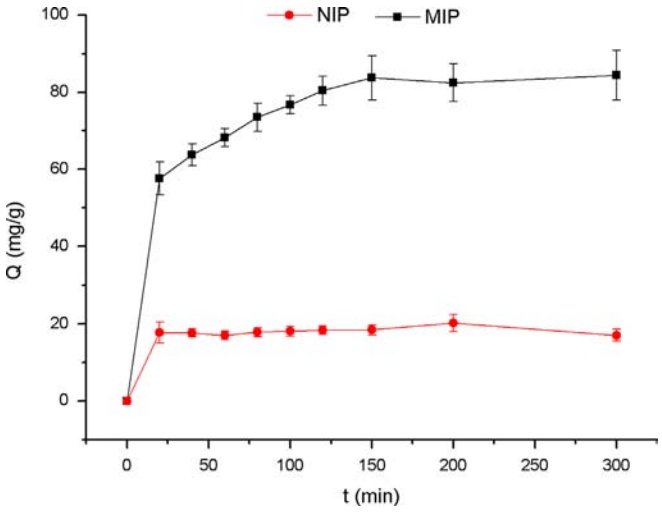

Fig. 9. Dynamic rebinding curves of BHb on Fe_3O_4@MIPs nanoparticles and Fe_3O_4@NIPs nanoparticles. Adsorption conditions: V=1 mL, m_{MIPs}=m_{NIPs}=10 mg, C_{BHb}=1.0 mg mL^{-1}, T=25 °C, t=0–300 min, pH=6.2.

3.4. Adsorption kinetics study

The rebinding kinetics was studied with an initial BHb concentration of 1.0 mg/mL. Fig. 9 shows the relationship of the adsorption capacity of MIPs (NIPs) and the adsorption time. We can find that the adsorption capacity of MIPs (NIPs) increases over time at first and then achieves a balance. For MIPs, within the first 20 min the adsorption capacity increases rapidly, from 20 min to 150 min, the adsorption rate becomes slower, and after 150 min reaches the adsorption plateau. We can speculate that when the adsorption process is just beginning, as there are many imprinted sites on the surface of the polymer the template protein can be easily combined with molecularly imprinted loci, so the adsorption capacity increases quickly. With the growth of time, more and

more imprinting sites were occupied, space steric hindrance became bigger, and the speed of template diffuses into molecular imprinted loci became slow. Finally the molecularly imprinted loci were fully occupied, and adsorption reached equilibrium.

NIPs reached a balance at an amazing speed – just 20 min. But the adsorption capacity is much smaller than that of the MIPs. This could be because there are adsorption cavities which are complementary to the template molecule in shape.

3.5. Selective adsorption experiments

The selectivity adsorption experiments of the imprinted nanoparticles were carried out with three other kinds of proteins: bovine serum albumin (BSA), ovalbumin (OVA), and lysozyme (Lyz). These three types of proteins were chosen to investigate the selectivity of the imprinted nanoparticles based on their molecular weights (MWs) and isoelectric points (pI). Compared to the template BHb, BSA has a similar MW but different pI. Both OVA and Lyz have different sizes and different pIs with BHb, but the pI of OVA is 4.7 (<7) while the pI of Lyz is 11.2 (>7). The selectivity adsorption experiment of MIP and NIP particles for four kinds of proteins was carried out with an initial concentration of 1.0 mg/mL, and the adsorption capacities of Fe_3O_4 @MIPs and Fe_3O_4@NIPs for different proteins are illustrated in Fig. 10. The imprinting factor and selectivity factor are shown in Table 2. It is not difficult to find that the MIP particles exhibited much higher selectivity for BHb ($IF_{BHb}=4.36$). BSA has nearly the same size with BHb; however, polymeric particles only have a little adsorption for it. This is determined by their different spatial structure. BHb is tetrameric protein composed of pairs of two different polypeptides and has a biconcave shape, while BSA is composed of a polypeptide and has an oval shape [37]. Hence its access to the imprinted cavities might be limited by the steric hindrance of polymer chains. Compared to BSA, polymeric particles showed a larger adsorption amount for OVA and Lyz. This is because they have smaller sizes than BHb, so the steric hindrance for their access to the imprinted cavities is relatively small. However, OVA and Lyz have different isoelectric points. OVA is negatively charged while Lyz is positively charged at pH 6.2. Since MIP nanoparticles were negatively charged, the electrostatic force between Lyz and the carboxyl group of the nanoparticles chains is impetus and makes it easy to distribute into the imprinted cavities. On the contrary, the electrostatic force between OVA and the carboxyl group of the nanoparticles chains is electrostatic repulsion, a hindering factor, and makes it easy to spread out the imprinted cavities. So Lyz has a relatively high adsorption capability.

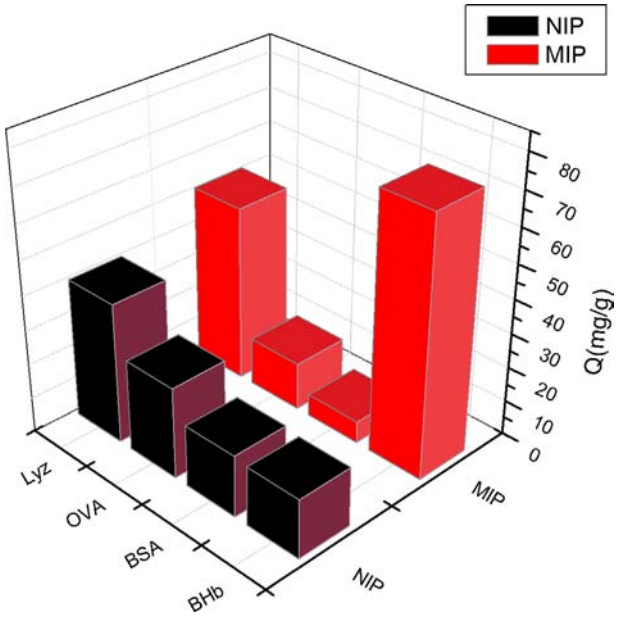

Fig. 10. Adsorption capacities of different proteins on Fe_3O_4@MIPs nanoparticles and Fe_3O_4@NIPs nanoparticles. Adsorption conditions: $V=1$ mL, $m_{MIPs}=m_{NIPs}=10$ mg, $C_0=1.0$ mg mL^{-1}, $T=25$ °C, $t=24$ h, pH=6.2.

Table 2
Results of the selectivity adsorption of Fe_3O_4@MIPs nanoparticles and Fe_3O_4@NIPs nanoparticles.

Parameter	BHb	BSA	OVA	Lyz
Imprinting factor (IF)[a]	4.36	0.36	0.52	1.26
Separation factor (R)[b]	–	12.11	8.38	3.46

[a] Imprinting factor (IF)=Q_{MIP}/Q_{NIP}.
[b] Separation factor (R)=IF(tem)/IF(ana), adsorption condition: $V=1$ mL, $m_{MIPs}=m_{NIPs}=10$ mg, $C_0=1.0$ mg mL^{-1}, $T=25$ °C, $t=24$ h, pH=6.2.

3.6. Competitive batch rebinding tests

To further determine the ability of the MIP nanoparticles, BSA was used as the competitor because it has a similar size as the template protein BHb. As seen in Fig. 11, most of the proteins adsorbed by the MIP were BHb, while the amount of BHb and BSA adsorbed by the NIP was close. At the same time, we can also find that the amount of BHb adsorbed by Fe_3O_4@MIPs in this case was lower than that observed in the batch rebinding tests. This is in conformity with the description in Ref. [19]. It is to say that imprinted cavities are formed successfully but the existence of competing proteins will suppress the adsorption for the template protein to some extent. Even so, the amount of BHb bound to Fe_3O_4@MIPs was still much larger than that of Fe_3O_4@NIPs with the imprinting factor of 2.30. Moreover, we performed the competitive batch rebinding SDS-PAGE analysis with the purpose of making the results more intuitive. In this system, ovalbumin was chosen as the competitive protein. Since bovine hemoglobin depolymerized under the action of SDS, so its corresponding stripe appears near the 14.4 kD. As seen in Fig. 12, most of the proteins adsorbed by the MIP were BHb, while both BHb and OVA were adsorbed by the NIPs. This result shows that Fe_3O_4@MIPs may be applicable to selectively separate BHb from a mixture of proteins.

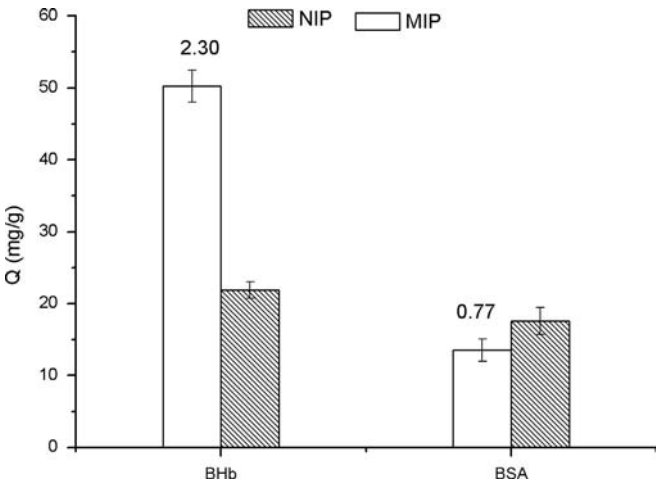

Fig. 11. Competive rebinding test of BHb and BSA on Fe_3O_4@MIPs nanoparticles and Fe_3O_4@NIPs nanoparticles. Adsorption conditions: $V=1$ mL, $m_{MIPs}=m_{NIPs}=10$ mg, $C_{0,BHb}=C_{0,BSA}=1.0$ mg mL^{-1}, $T=25$ °C, $t=24$ h, pH=6.2. The imprinting factors are marked above the bars.

3.7. Analytical performance

In order to test the performance of MIPs, five parallel experiments were carried out under optimal conditions. The results showed that the average adsorption capacity of the Fe_3O_4@MIPs was 71 mg g^{-1}, while that of Fe_3O_4@NIPs was 22 mg g^{-1}. The RSDs were 4.5% and 3.3%. It means that both the imprinted and non-imprinted nanoparticles have a relatively stable adsorption capacity to the BHb. So this approach is applicable to the rapid separation of BHb.

3.8. Real sample adsorption experiment

To test the practical applicability of MIPs, bovine calf serum was used as the real sample. As mentioned before, bovine hemoglobin depolymerized under the action of SDS, so its corresponding stripe appears near the 14.4 kD. The SDS-PAGE analysis (Fig. 13A.) shows that the eluate of MIPs exhibited a band with a molecular weight of ~14.4 kD, while there was no corresponding band in lane 7, the NIPs eluate. From Fig. 13B, we can see the color of MIPs eluate is deeper than that of NIPs eluate. These all proved MIPs have a better adsorption capability of BHb and it is potential in practical applications.

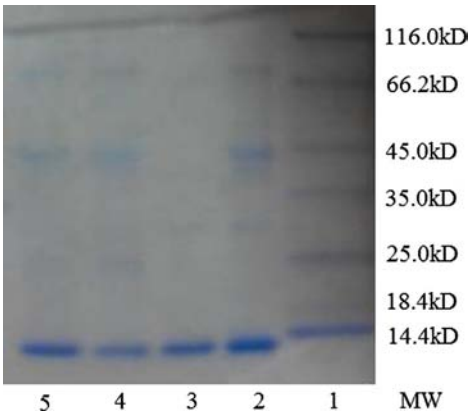

Fig. 12. The results of SDS-PAGE analysis for the isolation of BHb from a mixture solution. Lane 1, 10 μL of protein molecular weight marker; lane 2, 10 μL of protein mixture solution containing BHb and ovalbumin (each with a concentration of 1.0 mg mL^{-1}); lane 3, 10 μL of BHb solution (0.5 mg mL^{-1}); lane 4, 10 μL of mixture solution after the adsorption by the MIPs; lane 5, 10 μL of the mixture solution after adsorption by the NIPs.

3.9. The generality investigation of the method

Lysozyme was chosen as the template molecule to further investigate the generality of the proposed molecular imprinting method. The Lyz-imprinted nanoparticles were synthesized in the same way with the BHb-imprinted nanoparticles. In addition, the MIPs and NIPs without the addition of itaconic acid were also synthesized as control. From Fig. 14, we can find that those imprinted nanoparticles synthesized with IA have a higher template protein binding capacity than the control nanoparticles. In order to further investigate the imprinting effect of the Lyz-imprinted nanoparticles, the selectivity adsorption experiments were carried out with three other kinds of proteins, BSA, OVA and BHb. From Fig. 15, it was apparent that, the MIP particles exhibited a higher selectivity for Lyz with an IF of 1.33 and a specific adsorption capacity of 7.4 mg/g. Here, specific adsorption capacity is defined as the corresponding difference between the adsorption capacity of MIP and that of NIP. And it is another important parameter which is usually used to evaluate the imprinting effect of MIP. In addition, we can also find that the adsorption amount of

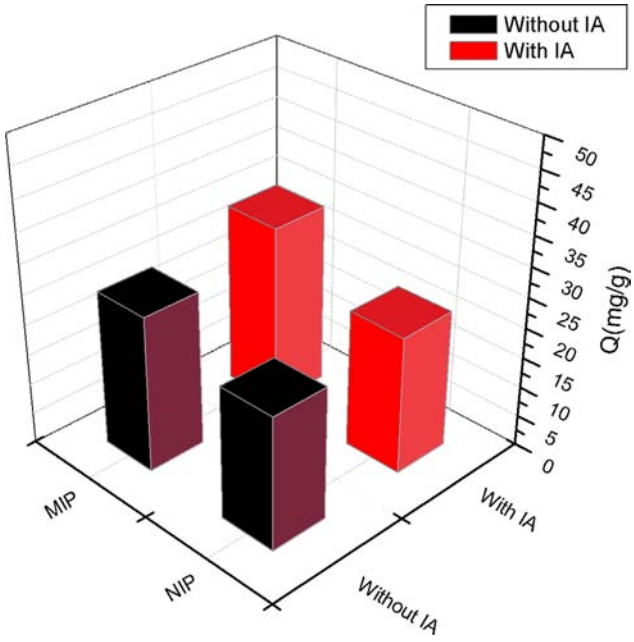

Fig. 14. The adsorption capacities of the Lyz-MIPs and Lyz-NIPs and the control group synthesized without IA. Adsorption conditions: V=1 mL, m_{MIPs}=m_{NIPs}=10 mg, C_{Lyz}=1.0 mg mL^{-1}, T=25 °C, t=24 h, pH=6.2.

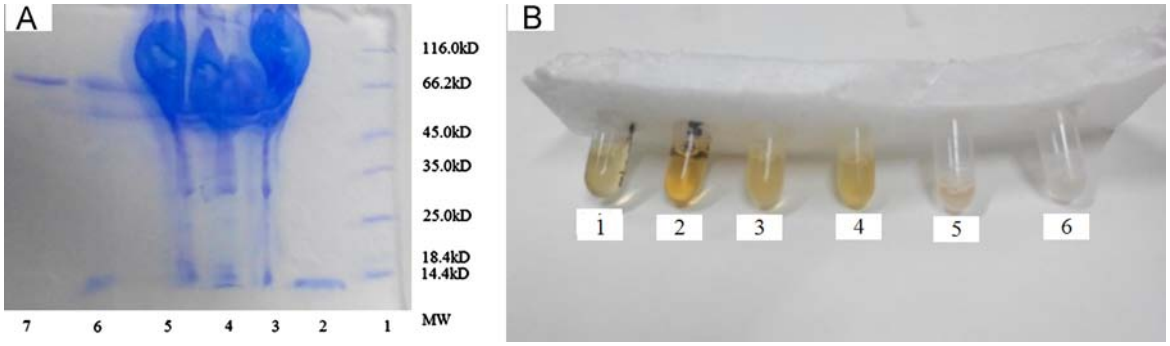

Fig. 13. A. The results of SDS-PAGE analysis for isolation of BHb from bovine calf serum. Lane 1, 10 μL of protein molecular weight marker; lane 2, BHb solution (0.5 mg mL^{-1}); lane 3, bovine calf serum before adsorption; lane 4, bovine calf serum after adsorption by the MIPs; lane 5, bovine calf serum after adsorption by the NIPs; lane 6, the MIPs eluate; lane 7, the NIPs eluate; B. The results of the isolation of BHb from bovine calf serum. 1, BHb solution (0.5 mg mL^{-1}); 2, bovine calf serum before adsorption; 3, bovine calf serum after adsorption by the MIPs; 4, bovine calf serum after adsorption by the NIPs; 5, the MIPs eluate; 6, the NIPs eluate.

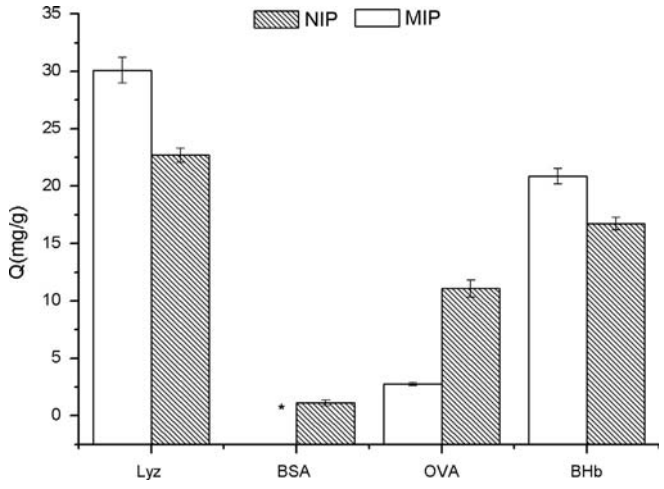

Fig. 15. Adsorption capacities of different proteins on Lyz-MIPs and Lyz-NIPs. Adsorption conditions: $V=1$ mL, $m_{MIPs}=m_{NIPs}=10$ mg, $C_0=1.0$ mg mL^{-1}, $T=25$ °C, $t=24$ h, pH=6.2. * denotes too little to be detected.

BSA and OVA on the MIP particles was small, while that of BHb was relatively high. This result also verified that the MIP particles were negatively charged as BSA and OVA molecules at pH 6.2.

4. Conclusions

In summary, a new type of BHb-imprinted magnetic nanoparticles was synthesized in the presence of monomer (IA) and a basic monomer (AAm). The research showed that the adsorption capacity of Fe_3O_4@MIPs was as high as 77.6 mg g^{-1}, while the adsorption capacity of Fe_3O_4@NIPs, which were prepared at the same conditions just without the template proteins, was significantly lower in all cases. Moreover, Fe_3O_4@MIPs exhibited significant specificity for BHb. The high adsorption capacity and selectivity factors proved that special recognition sites which are sterically complementary to the template molecules BHb were formed in the process of preparation. The easy preparation, fast mass transfer rate, easy separation and high selectivity to the template protein BHb make this approach applicable to the rapid separation of BHb.

Acknowledgments

The authors greatly appreciate the financial supports by the National Natural Science Foundation of China (Nos. 21175040, 21375035, and J1210040) and the Foundation for Innovative Research Groups of NSFC (Grant 21221003).

References

[1] D.F. Tai, M.H. Jhang, G.Y. Chen, S.C. Wang, K.H. Lu, Y.D. Lee, H.T. Liu, Anal. Chem. 82 (2010) 2290–2293.
[2] J.P. Li, Y.P. Li, Y. Zhang, G. Wei, Anal. Chem. 84 (2012) 1888–1893.
[3] C.G. Xie, H.F. Li, S.Q. Li, J. Wu, Z.P. Zhang, Anal. Chem. 82 (2010) 241–249.
[4] B.W. Wu, Z.H. Wang, D.X. Zhao, X.Q. Lu, Talanta 101 (2012) 374–381.
[5] Z.H. Wang, H. Li, J. Chen, Z.H. Xue, B.W. Wu, X.Q. Lu, Talanta 85 (2011) 1672–1679.
[6] E. Caro, R.M. Marce, P.A.G. Cormack, D.C. Sherrington, F. Borrull, Anal. Chim. Acta 562 (2006) 145–151.
[7] T.H. Jiang, L.X. Zhao, B.L. Chu, Q.Z. Feng, W. Yan, J.M. Lin, Talanta 78 (2009) 442–447.
[8] Y.L. Hu, Y.W. Li, R.J. Liu, W. Tan, G.K. Li, Talanta 84 (2011) 462–470.
[9] N.M. Bergmann, N.A. Peppas, Prog. Polym. Sci. 33 (2008) 271–288.
[10] B. Sellergren, C.J. Allender, Adv. Drug Deliv. Rev. 57 (2005) 1733–1741.
[11] Q.Q. Gai, F. Qu, Z.J. Liu, R.J. Dai, Y.K. Zhang, J. Chromatogr. A 1217 (2010) 5035–5042.
[12] Q.Q. Gai, F. Qu, T. Zhang, Y.K. Zhang, J. Chromatogr. A 1218 (2011) 3489–3495.
[13] T. Jing, H.R. Du, Q. Dai, H. Xia, J.W. Niu, Q.L. Hao, S.R. Mei, Y.K. Zhou, Biosens. Bioelectron. 26 (2010) 301–306.
[14] G.Q. Fu, H.Y. He, Z.H. Chai, H.C. Chen, J. Kong, Y. Wang, Y.Z. Jiang, Anal. Chem. 83 (2011) 1431–1436.
[15] H.Y. He, G.Q. Fu, Y. Wang, Z.H. Chai, Y.Z. Jiang, Z.L. Chen, Biosens. Bioelectron. 26 (2010) 760–765.
[16] B.J. Gao, H.Y. Fu, Y.B. Li, R.K. Du, J. Chromatogr. B 878 (2010) 1731–1738.
[17] X.P. Jia, M.L. Xu, Y.Z. Wang, D. Ran, S. Yang, M. Zhang, Analyst 13 (2013) 651–658.
[18] C.J. Tan, Y.W. Tong, Anal. Chem. 79 (2007) 299–306.
[19] C.J. Tan, H.G. Chua, K.H. Ker, Y.W. Tong, Anal. Chem. 80 (2008) 683–692.
[20] A. Bossi, S.A. Piletsky, E.V. Piletska, P.G. Righetti, A.P.F. Turner, Anal. Chem. 73 (2001) 5281–5286.
[21] H. Nishino, C.S. Huang, K.J. Shea, Angew. Chem. Int. Ed. 45 (2006) 2392.
[22] D.F. Tai, C.Y. Lin, T.Z. Wu, L.K. Chen, Anal. Chem. 77 (2005) 5140.
[23] L. Qin, X.W. He, W. Zhang, Y.K. Zhang, Anal. Chem. 81 (2009) 7206–7216.
[24] A. Uysal, G. Demirel, E. Turan, T. Caykara, Anal. Chim. Acta 625 (2008) 110–115.
[25] Z.D. Hua, Z.Y. Chen, Y.Z. Li, M.P. Zhao, Langmuir 24 (2008) 5773–5780.
[26] D. Ran, Yuzhi Wang, Xiaopin Jia, C. Nie, Anal. Chim. Acta 723 (2012) 45–53.
[27] T.Y. Guo, Y.Q. Xia, J. Wang, M.D. Song, B.H. Zhang, Biomaterials 26 (2005) 5737–5745.
[28] T.Y. Guo, Y.Q. Xia, G.J. Hao, B.H. Zhang, Chin. Chem. Lett. 15 (2004) 1339–1341.
[29] F. Li, J. Li, S.S. Zhang, Talanta 74 (2008) 1247–1255.
[30] I.J. Bruce, J. Taylor, M. Todd, M.J. Davies, E. Borioni, C. Sangregorio, T. Sen, J. Magn. Magn. Mater. 284 (2004) 145–160.
[31] F.W. Scheller, N. Bistolas, S.Q. Liu, M. Janchen, M. Katterle, U. Wollenberger, Adv. Colloid Interface 116 (2005) 111–118.
[32] Y.Q. Wang, H.M. Zhang, Q.H. Zhou, Eur. J. Med. Chem. 44 (2009) 2100–2105.
[33] X.J. Song, W. Gong, J. Wang, Chemistry 07 (2005) 504–509.
[34] B.Y. Huang, Y.C. Chen, G.R. Wang, C.Y. Liu, J. Chromatogr. A 1218 (2011) 849–855.
[35] C. Lopez, B. Claude, Ph Morin, J.-P. Max, R. Pena, J.-P. Ribet, Anal. Chim. Acta 683 (2011) 198–205.
[36] B. Feng, Z.Q. Ren, J.M. Qu, R.Y. Hong, H.Z. Li, D.G. Wei, New Chem. Mater. 36 (2008) 26–28.
[37] Y.Q. Xia, T.Y. Guo, H.L. Zhao, M.D. Song, B.H. Zhang, B.L. Zhang, J. Biomed. Mater. Res. 90 (2009) 326–332.